Soft Photon Theorem in QCD with Massless Quarks

Yao Ma,[1,*] George Sterman,[2,†] and Aniruddha Venkata[2,‡]
[1]Insitute for Theoretical Physics, ETH, 8093 Zurich, Switzerland
[2]C.N. Yang Institute for Theoretical Physics and Department of Physics and Astronomy, Stony Brook University, Stony Brook, New York 11794–3840, USA

(Received 8 December 2023; revised 29 January 2024; accepted 1 February 2024; published 28 February 2024)

Working to all orders in dimensionally regularized QCD with massless quarks, we study the radiation of a photon whose energy is much lower than that of external partons. The conventional soft photon theorem receives corrections at leading power in the photon energy, associated with soft virtual loops of massless fermions. These additive corrections give an overall factor times the nonradiative amplitude that is infrared finite and real to all orders in α_s. Based on recent calculations of the three-loop soft gluon current, we identify the lowest-order three-loop correction.

DOI: 10.1103/PhysRevLett.132.091902

Electromagnetic radiation in the scattering of charged particles through the strong interactions is described at low energy $\omega(k)$ by the celebrated soft photon theorem, which determines the first two powers of $\omega(k)$ in terms of the nonradiative amplitude [1–5]. For all charged particles massive, the amplitude M_{a+1} to emit a photon with sufficiently small energy $\omega(k)$ and polarization $\epsilon(k)$ is given schematically by

$$M_{a+1}\left[\{p_i\},k,\epsilon(k)\right]=\sum_{i=1}^{a}\delta_i e_i\frac{p_i^\mu}{p_i\cdot k}\left[\epsilon_\mu(k)-(k_\mu\epsilon^\nu(k)-\epsilon_\mu(k)k^\nu)O_\nu(p_i,k)\right]M_a(\{p_i\}),\quad(1)$$

with M_a the nonradiative amplitude and $\delta_i=+1$ (-1) for particle i with charge e_i outgoing (incoming). In the correction term, M_a is acted on by a momentum-dependent operation $O_\nu(p_i,k)$ [5–7] that does not change the power of k. Working in QCD, we will study soft photon production in pair creation processes: singlet $\to f(p_1)+\bar{f}(p_2)$, for particles with electromagnetic charges $\pm e_f$. We will be concerned primarily with the leading power, but extensions of the reasoning below can be applied to the first power correction as well. We will always assume a fixed angle of order unity between the photon and either of the charged particles.

As extended by Gribov [3] and Del Duca, [5], Eq. (1) holds for fixed-angle radiation so long as $\omega(k)\ll m$, the mass of any charged particle. With this assumption, Eq. (1) applies quite generally, and specifically for dimensionally regularized perturbative amplitudes for QCD with massive quarks. In this Letter, we show that for pair creation or annihilation in *massless* QCD, or when the photon energy exceeds the masses of some quarks, the relation Eq. (1) receives corrections that are of leading power $1/\omega(k)$. Specifically, we will show that for the pair production amplitude of flavor f, keeping leading power only, with n_0 massless quark flavors,

$$M_3^{(f)}[\{p_i\},k,\epsilon(k)]=\left[e_f+\Gamma_{\rm EM}^{(f)}(\alpha_s)\left(\sum_{n=1}^{n_0}e_n\right)\right]\times\left[\frac{p_1\cdot\epsilon(k)}{p_1\cdot k}-\frac{p_2\cdot\epsilon(k)}{p_2\cdot k}\right]M_2^{(f)}(\{p_i\}).\quad(2)$$

Here, $\Gamma_{\rm EM}^{(f)}(\alpha_s)$, which we will refer to as the soft photon factorization constant, is an infrared finite expansion in the strong coupling. It comes from loops of massless quarks (charges e_n), and begins at order α_s^3. The corresponding contribution when $\omega(k)\ll m$ appears in the subleading term in Eq. (1). This additive correction in Eq. (2) is independent of the electromagnetic charges of the external particles, but is sensitive to their color representations. As a result of gauge invariance, the tensor structure of the correction matches that of the familiar form Eq. (1). In principle, $\Gamma_{\rm EM}^{(f)}$ may also be a function of the external momenta, but as we shall see, it is independent of momenta at lowest order in four dimensions. We will extract the explicit value of $\Gamma_{\rm EM}^{(f)}$ at lowest nonvanishing order from the explicit calculation of the soft gluon current in Refs. [8] and [9] using a method we describe below. A corresponding result holds as well for massless quantum

electrodynamics, with an analogous $\Gamma_{\rm EM}$ beginning at α^3. This gauge invariant contribution is additional to the classic leading terms in Eq. (1), which have been derived in recent years for massless QED from asymptotic symmetry considerations [10].

Our discussion starts with the identification of regions of loop momentum space in diagrams that contribute to the amplitude $M_3^{(f)}$ and that are leading in both the large scale of the process and the smaller scale of the photon energy. Infrared, mass-sensitive behavior arises only where loop momenta are pinched by propagator poles, called pinch surfaces in Ref. [11].

For the exclusive amplitude, $M_2^{(f)}(p_1, p_2)$, the pinch surfaces are uniquely identified by subsets of lines that either are on shell and collinear to external on-shell particles (jet subdiagrams) or have vanishing momenta (soft subdiagram), with the remaining lines off shell (hard subdiagram) [12–14]. Straightforward power counting shows that singularities of the exclusive amplitude are logarithmic [11]. Factorized forms of the exclusive amplitudes in terms of jet, hard, and soft functions, $M_2 = H\,J_1\,J_2\,S$, are well established in direct QCD [13–19] and soft-collinear effective theory [20,21]. We will follow the matrix element conventions for the jet functions J_i in Ref. [16], in which soft singularities are subtracted from the jet functions to avoid double counting with the soft function.

Turning to the radiative amplitude $M_3^{(f)}$ because the photon energy is small compared to the momenta of the external charged particles, the leading, $\mathcal{O}[1/\omega(k)]$ behavior can only arise in loop momentum configurations where the soft photon emerges either from (anti)quarks in the jet subdiagrams, collinear to the external particles, or from soft fermion loops in the soft subdiagram. These contributions, which are additive, are illustrated in Figs. 1(a) and 1(b), respectively. In both cases, soft quanta, including those that carry the momentum of the photon, factor from jet subdiagrams at leading power in center-of-mass energy. Soft-jet-hard factorization, which occurs in every leading region, applies to the radiative amplitude $M_3^{(f)}$ just as for the exclusive amplitude $M_2^{(f)}$. In the factorized forms of both the exclusive and radiative amplitudes, the soft function is given by the products of Wilson lines in the directions $\beta_i \propto p_i$, $\Phi_{\beta_i}^{(R_i)}(0) = P\,\exp[\int_0^\infty d\lambda(-ig_s)\beta_i \cdot A^{(R_i)}(\beta_i\lambda)]$, in the color representations R_i of the external particles [13–21]. We note that the radiative soft function S in Fig. 1(b) has additional pinch surfaces due to the presence of the external photon, as we discuss below.

Based on the structure of both jet and soft loop emissions, the external soft photon enjoys further factorization properties. If it attaches to a jet, the factorization is illustrated by Fig. 2(a). The contributions of all quark loops within the jet cancel [3,5], and the soft photon is sensitive only to the charge and velocity of the external particle. At leading power, this factorization gives the multiplicative eikonal factor represented by the double line and contributes to the e_f term in Eq. (2).

In contrast, if the external soft photon attaches to the soft subdiagram, the factorization is illustrated in Fig. 2(b), where the soft photon contribution factors into the product of the soft function of the elastic amplitude $M_2^{(f)}$, times a diagram W coupled by gluons to the product of Wilson lines. To avoid double counting, these Wilson lines do not couple to the photon field. The soft function with single-photon emission is the Fourier transform of the matrix element $\langle 0|T(\Phi_{\beta_2}^{(\bar{f})}(0)\epsilon \cdot j_{\rm EM}(y)\Phi_{\beta_1}^{(f)}(0)|)0\rangle$, in terms of the electromagnetic current operator $j_{\rm EM}$ and the Wilson lines $\Phi^{(f)}$ defined above. As we will see below, this factorization comes about as a consequence of the exponentiation properties of products of Wilson lines (a single cusp for our case), resulting in the $\Gamma_{\rm EM}^{(f)}$ term in Eq. (2).

The exponentiation analysis of products of Wilson lines joined at a cusp [22–27], see particularly Ref. [28], applies unchanged if we supplement the Lagrange density of massless QCD by a vertex that couples quarks to a background electromagnetic field through the normal quark electromagnetic currents. If we take that field to be a plane wave of momentum k with a corresponding polarization vector $\epsilon(k)$ the resulting soft function is an expansion of the

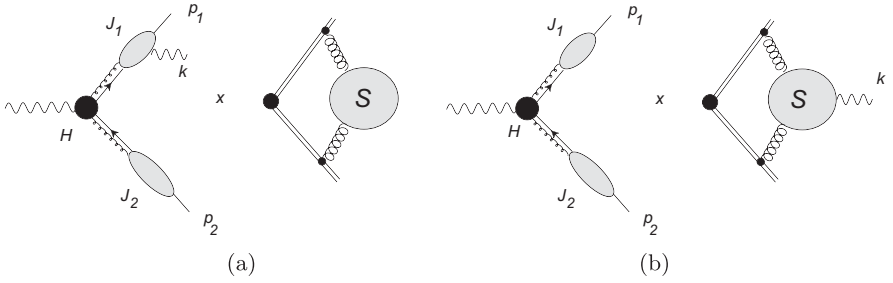

FIG. 1. Leading regions for the soft photon emission amplitude $M_3^{(f)}$, after factorization of soft lines from jets: (a) radiation from jets (J_i) associated with external lines, (b) radiation from fermion loops in soft subdiagram S. H represents the hard subdiagram. The gluon lines in the figure represent arbitrary numbers of propagators connected to the Wilson lines or hard subdiagram. The leading regions for the elastic process $M_2^{(f)}$ lack the photon, but are otherwise identical.

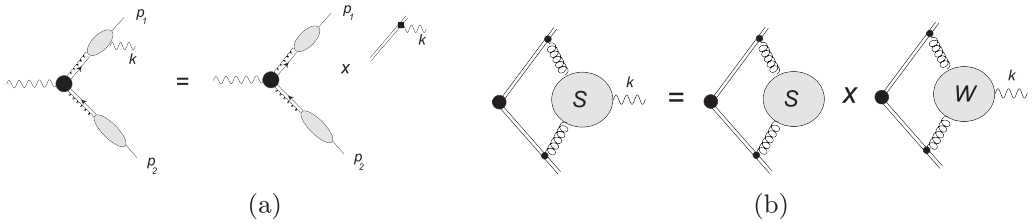

FIG. 2. Factorization of the soft photon: (a) as eikonal factor from jet(s), (b) as part of a single radiative web, W from the soft part, Eq. (6). The gluon lines represent arbitrary numbers of soft or collinear connections in the general case.

general form, in $\varepsilon = 2 - D/2$ dimensions, in terms of velocities $\beta_{1,2}$,

$$\bar{S}^{(f)}[\beta_1,\beta_2,k,\epsilon(k),\alpha_s,e,\varepsilon] = \sum_{i,j}\left(\frac{\alpha_s}{\pi}\right)^i e^j\,\bar{S}^{(f)}_{(i,j)}\left[\beta_1,\beta_2,k,\epsilon(k),\varepsilon\right], \tag{3}$$

where i and j count the order in α_s and the unit electromagnetic charge e, and therefore the loop order and the number of photon couplings, respectively. Our interest is entirely in the linear order in e, which by itself obeys the QED Ward identity, vanishing when $\epsilon^\mu(k) \propto k^\mu$. The complete sum, however, possesses the same diagrammatic exponentiation properties as QCD. This is because the construction of the exponent depends only on analyzing attachments of the gluon field to the Wilson lines, and not at all on the remainder of the diagrams to which the gluons couple [22–28].

The result of this analysis applied to the singlet cusp is that the sum of all diagrams takes an exponential form in terms of so-called web diagrams, which are constructed recursively as combinations of crossed and connected diagrams coupled to Wilson lines, with modified color factors. In this case, the web functions themselves can be expanded in the electromagnetic charge as well as the strong coupling, at renormalization scale μ in D dimensions as

$$\bar{S}^{(f)}[\beta_1,\beta_2,k,\epsilon(k),\alpha_s,e,\varepsilon] = \exp\left[\int\frac{d^Dl}{(2\pi)^D}\frac{\beta_1\cdot\beta_2}{l\cdot\beta_1\, l\cdot\beta_2}\frac{1}{l^2}\sum_{i,j}\left(\frac{\alpha_s(\mu,\varepsilon)}{\pi}\right)^i e^j\, w^{(f)}_{(i,j)}(\{\beta_i\},l,\mu,k,\epsilon(k),\varepsilon)\right], \tag{4}$$

where all loop integrals internal to the web diagrams $w^{(f)}_{(i,j)}$ have been carried out, leaving only the loop l that joins the web with the cusp vertex. Factoring an explicit $1/l^2$ as shown, the web functions are dimensionless. Note that the functions $w^{(f)}_{(i,0)}$ do not depend on k and $\epsilon(k)$. In the following, we refer to the function $w^{(f)}_{(i,1)}$ in Eq. (4) as the ith order radiative web function.

The web functions in Eq. (4), which are integrated over their internal momenta at fixed l, are renormalization-scale independent in the strong coupling [22,23], while the background photon field is unrenormalized. Thus at fixed j,

$$\mu\frac{d}{d\mu}\sum_i\left(\frac{\alpha_s(\mu,\varepsilon)}{\pi}\right)^i e^j\, w^{(f)}_{(i,j)}(\{\beta_i\},l,\mu,k,\epsilon(k),\varepsilon) = 0. \tag{5}$$

In addition, the web functions at every order are free of soft and collinear singularities when subsets of lines have vanishing momenta or become collinear to the velocities β_1 or β_2. This property [29], which follows from the web construction, as explained in Ref. [30], is inherited by the focus of our interest, the linear term in the electromagnetic charge, which is found simply by expanding the exponent of Eq. (4),

$$\begin{aligned}\bar{S}^{(f)}_1\left[\beta_1,\beta_2,k,\epsilon(k),\alpha_s,e,\varepsilon\right] &= e^{\int\frac{d^Dl}{(2\pi)^D}\frac{\beta_1\cdot\beta_2}{l\cdot\beta_1\, l\cdot\beta_2}\frac{1}{l^2}\sum_{i=1}^{\infty}\left(\frac{\alpha_s(\mu,\varepsilon)}{\pi}\right)^i w^{(f)}_{(i,0)}(\{\beta_i\},l,\mu,\varepsilon)}\\ &\times\int\frac{d^Dl}{(2\pi)^D}\frac{\beta_1\cdot\beta_2}{l\cdot\beta_1\, l\cdot\beta_2}\frac{1}{l^2}\\ &\times\sum_{i=3}^{\infty}\alpha_s^i(\mu,\varepsilon)e\, w^{(f)}_{(i,1)}(\{\beta_i\},l,\mu,k,\epsilon(k),\varepsilon).\end{aligned} \tag{6}$$

The first factor on the right is the unrenormalized soft function for the nonradiative QCD process [16], given by the exponential of the sum of pure QCD webs, $w^{(f)}_{(i,0)}$ in Eq. (4). The renormalization of integral l for the $w^{(f)}_{(i,0)}$ webs in the exponent defines the soft function for $M^{(f)}_2$ [16]. The second factor in Eq. (6) has all the dependence on k and $\epsilon(k)$. Its integral over l is ultraviolet finite. It satisfies the QED Ward identity independently, and hence must take the form,

$$\begin{aligned}&\int\frac{d^Dl}{(2\pi)^D}\frac{\beta_1\cdot\beta_2}{l\cdot\beta_1\, l\cdot\beta_2}\frac{1}{l^2}\sum_{i=3}^{\infty}\alpha_s^i(\mu,\varepsilon)e\, w^{(f)}_{(i,1)}(\{\beta_i\},l,\mu,k,\epsilon(k),\varepsilon)\\ &= \Gamma^{(f)}_{\rm EM}(\alpha_s)\left(\sum_{n=1}^{n_0}e_n\right)\left[\frac{\beta_1\cdot\epsilon(k)}{\beta_1\cdot k}-\frac{\beta_2\cdot\epsilon(k)}{\beta_2\cdot k}\right],\end{aligned} \tag{7}$$

where in the prefactor, $\Gamma^{(f)}_{\rm EM}(\alpha_s)$, any residual dependence on momenta is suppressed. We also drop dependence of $\Gamma^{(f)}_{\rm EM}(\alpha_s)$ on ε here, because, as we argue below, both the integrand and the integral on the left-hand side of this expression are finite in four dimensions.

Using Eq. (7) in Eq. (6), renormalizing the soft function and multiplying by the jet and hard functions, we derive the second term in the soft photon theorem for massless QCD, Eq. (2). This is the primary result of our analysis. We emphasize at the outset that the $1/\omega(k)$ behavior of the right-hand side is entirely due to loops of massless quarks. For photon energies below the scales of nonzero quark masses, the coupling of a photon to the corresponding quark loop is suppressed by the ratio $\omega(k)/m$, and appears in the power correction term in Eq. (1). A study of the turnover between these two regimes will certainly be of interest.

The web diagrams in Eq. (7) are represented schematically on the right of Fig. 2(b). Because of color and charge conjugation invariance, the lowest nonvanishing order for the soft-photon web is α_s^3, illustrated in Fig. 3(a). The three-loop eikonal diagram shown in Fig. 3(a) and the general radiative web functions on the right of Fig. 2(b) are proportional to $1/\omega(k)$ after the integral over l in Eq. (7). This behavior is characteristic of the "soft" region where all components of momentum in the three loops are of order $\omega(k)$. This can be verified readily by standard power counting for soft singularities, as described, for example, in Ref. [11].

To verify that the coefficient $\Gamma^{(f)}_{\rm EM}$ is infrared finite, we must confirm that the complete radiative web has no infrared divergences in four dimensions, even though its individual diagrams have many leading power pinch surfaces. In Fig. 3(b), we show a typical leading pinch surface for a radiative web. Subsets of virtual lines form jet subdiagrams (shaded) collinear to the p_1, p_2, or k directions, with other lines, labeled W', soft in all components relative to the momenta of the jet subdiagrams. Note that the soft subdiagram W' is connected to jets only through gluon lines. Momentum configurations where a fermion loop appears in both jet and soft subdiagrams are always suppressed compared to leading power [11]. The fermion loop to which the photon connects must therefore be entirely in one of the k, p, or p' jets, or in the soft function. Individual graphical contributions to $\Gamma^{(f)}_{\rm EM}$ inherit poles up to $1/\epsilon^5$ for diagrams at $\mathcal{O}({\alpha_s}^3)$ from the general configurations illustrated by Fig. 3(b), and every higher order of α_s increases the power of ε by two.

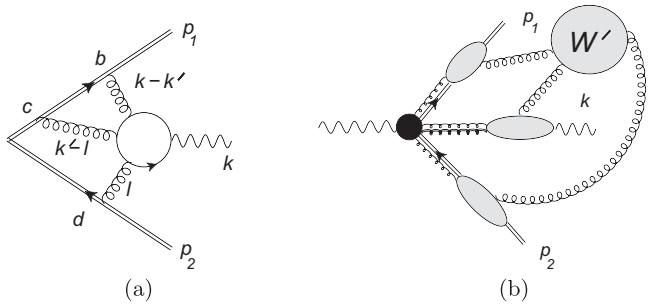

FIG. 3. (a) Representative α_s^3 quark-loop photon emission diagram for the soft function of the radiative pair creation process, with assigned gluon momenta. Loop momentum l joins the cusp and the web subdiagram as in Eq. (6). Color indices b, c, and d, which link the fermion loop and Wilson lines, are discussed in the text. (b) Most general pinch surface for individual diagrams that contribute to the radiative web function, $w^{(f)}_{(i,1)}$. Here, the double straight lines represent the Wilson lines and the double gluon lines, gluons carrying physical polarization. All other gluon lines represent arbitrary numbers of connections. In the sum of web diagrams, all collinear singularities associated with jet subdiagrams on the p_1 and p_2 lines cancel.

We first show how, after combining diagrams, all leading-power singularities associated with nontrivial p_1 and p_2 jets cancel. In diagrams like Fig. 3(a), and indeed at any order, if the momentum of the quark loop reaches a scale much larger than k and is collinear to p_1 or p_2, the diagrams found by connecting photon k to the loop in all ways cancel by the QED Ward identity [3,5]. At high orders, leading pinch surfaces like those shown in Fig. 3(b) do occur, in which the p_1 and p_2 Wilson lines are accompanied by collinear jet subdiagrams connected to the remainder of the on-shell diagram by soft gluon lines. As noted above, however, such singularities cancel in the sum of web diagrams at any order.

In the remaining leading pinch surfaces in Fig. 3, the entire fermion loop is part of a virtual jet of lines collinear to the photon. This is an unusual jet, however, because although it originates at the Wilson line as a set of collinear gluons, its entire momentum reaches the final state as a color-singlet photon [31]. Such a jet can be factored from the Wilson line, in the same manner as the jets of the form factor. At the same time, soft gluons also can be factored from this jet [13–21], coupling only to a Wilson line in adjoint representation and in the direction of momentum k. These soft gluons would multiply a gauge invariant jet subdiagram that describes a gluon (with physical polarization) at short distances yet evolves without radiation into a single photon final state. Such a matrix element would vanish by color conservation. This ensures the cancellation of infrared poles associated with gluons much softer than $\omega(k)$ at such leading pinch surfaces, and, consequently, the infrared finiteness of $\Gamma^{(f)}_{\rm EM}(\alpha_s)$.

Given the complexity of the diagrams involved, with poles up to $1/\epsilon^5$ in individual diagrams, the lowest nonvanishing order is already a strong test of the reasoning above. Remarkably, very recent calculations in massless QCD include precisely this quantity, up to an overall shift in color factor. References [8] and [9] both calculate the diagrams of the type shown in Fig. 3(a), but with an external gluon rather than photon, as part of the much larger

calculation of the soft gluon current. For an external gluon, these diagrams have poles in dimensional regularization up to $1/\varepsilon^6$ in their dominant color structure. At this order, however, a maximally symmetric color factor appears, equal to $(1/4!)\mathrm{Tr}[T^aT^bT^cT^d + \text{permutations}]$, with generators T^i in the fundamental representation. [Comparing to Fig. 3(a), the external gluon would have color index a.] This color structure is present in every diagram like Fig. 3(a), with three gluons connecting the fermion loop to the Wilson lines, and only in those diagrams.

We now observe that the subset of gluon emission diagrams that provide the maximally symmetric color tensor are in one-to-one correspondence to diagrams in the *full* set of diagrams for radiation of a photon. After using charge conjugation invariance, the surviving color factor from each quark loop diagram for photon emission is proportional to the symmmetric tensor $(1/4)d^{bcd} = (1/2)\mathrm{Tr}[T^bT^cT^d + T^dT^cT^b]$. For both gluon and photon emission, the result of the quark loop color trace is contracted with the same color generators, $T^e_{(R_f)}$, $e = b,\ c,\ d$, on the Wilson lines, whose relative order depends on the diagram in question, but whose product is invariant under permutations because of the symmetry of the traces. The sets of gluon- and photon-radiative diagrams are thus related by the ratio of their respective color factors and the substitution of an electromagnetic charge e_n for one power of g_s. This procedure gives for the radiative coefficients with external quarks of flavor $f = F$,

$$\Gamma^{(F)}_{\mathrm{EM}} = -\left(\frac{\alpha_s}{\pi}\right)^3 C_F^{(3)}\left(-\frac{\zeta_2}{2} + \frac{\zeta_3}{6} + \frac{5\zeta_5}{6}\right), \tag{8}$$

where $C_F^{(3)}$ is the cubic Casimir of the $SU(n)$ Lie algebra, $C_F^{(3)} = d^{bcd}T_F^bT_F^cT_F^d$ in the fundamental representation. The corresponding coefficient vanishes for the gluon, $T_F \to T_A$. Analogous reasoning shows that the same formula holds for massless QED, with the substitutions $C_F^{(3)} \to 4$ and $\alpha_s \to \alpha$. Unlike the familiar soft photon theorem terms in Eq. (2), the $\Gamma^{(f)}_{\mathrm{EM}}$ contribution depends directly on the color representations of external particles $f, \bar{f}$, rather than on their electromagnetic charges.

In summary, for the α_s^3 diagrams of Fig. 3(a) and at higher orders, the integrals that determine the soft photon factorization constant are free of subdivergences, giving $1/\omega(k)$ times an infrared finite number. As a result, all logarithms in the expansion of $\Gamma^{(f)}_{\mathrm{EM}}$ can only have arguments depending on $\omega(k)/\mu$. Then the renormalization scale invariance of the web, Eq. (5), implies that the scale of the running coupling in $\Gamma^{(f)}_{\mathrm{EM}}$ is naturally chosen as $\omega(k)$. Indeed, in the order α_s^3 results of Refs. [8,9], at higher orders in the ε expansion, logarithms appear with argument $(p_1\cdot k)(p_2\cdot k)/(p_1\cdot p_2\mu^2) \sim (\omega(k)/\mu)^2$.

A striking feature of Eq. (8) is that $\Gamma^{(f)}_{\mathrm{EM}}(\alpha_s)$ is a real number in four dimensions, even though intermediate states found by cutting diagrams like Fig. 3(a) can clearly go on shell. The creation of an on-shell intermediate state requires, however, momentum transfer between the light-like eikonal lines. In a causal theory, this can only occur at short distances, or through collinear emission, both inconsistent with $1/\omega(k)$ behavior. To check this in perturbation theory, consider in Fig. 3(a) the state consisting of two on-shell eikonal lines and gluon $k' - l$. In the region that gives this cut, gluon $k - k' \equiv k_1$ must satisfy $p_1\cdot k_1 = p_1^+k_1^- = 0$, where we take p_1 in the light-cone plus direction. We can now construct a path that passes through gluon k_1 and then through a sequence of vertices and lines, always against the flow of positive minus momentum. This sequence avoids the photon line, which carries momentum out of the diagram. It must eventually reach either the p_1 or p_2 eikonal line, along which it can be completed back to the k_1 line as a loop. By construction, the plus momentum flowing around this loop has poles only in the upper half plane. As a result, we may deform this plus loop momentum to any large scale, and all lines in the loop will be either far off shell or will be absorbed into the p_1 jet. But we have seen that both at order α_s^3 and beyond, such momentum configurations do not contribute at order $1/\omega(k)$. An analogous construction applies to any pole on an eikonal line in any diagram contributing to $\Gamma^{(f)}_{\mathrm{EM}}$, and therefore to any on-shell intermediate state. Our factorization constant is thus real to all orders.

Equation (2) is of interest in its own right as a result in massless QCD and related gauge theories. Since it is well defined at zero quark mass, it should also hold approximately for masses small compared to the photon energy. This suggests that the coefficient of the $1/\omega(k)$ behavior of the amplitude for soft photon emission changes with the photon energy. For $\omega(k)$ small enough, it is given by the classic formula, Eq. (1) in terms of the charges of external particles, but as the energy increases past the masses of charged fermions, new $1/\omega(k)$ contributions appear. Indeed, to capture the complete $1/\omega(k)$ asymptotic behavior at very high energies for the exclusive process, we can take the number of massless quark flavors n_0 to count all quark masses less than $\omega(k)$. This quantitative but formal result may have indirect phenomenological consequences. It may, for example, provide a link between perturbative analysis of amplitudes and the nonperturbative model analyses [32–36] that have been proposed to explain the apparent excess of relatively soft photon emission in a variety of experiments [37–39]. Clearly, at the perturbative level, it will be interesting to explore possible implications of this analysis for the scattering of bound states, both charged and neutral. Other interesting generalizations of these results will be to more external colored particles [19,40,41], more external photons, and the next power in photon momentum.

We thank Charalampos Anastasiou, Franz Herzog, Eric Laenen, Lorenzo Magnea, and Bernhard Mistlberger for very helpful discussions. This work was supported by the National Science Foundation, Grants No. PHY-1915093 and No. PHY-2210533.

*yaomay@phys.ethz.ch
†george.sterman@stonybrook.edu
‡aniruddha.venkata@stonybrook.edu

[1] F. E. Low, Bremsstrahlung of very low-energy quanta in elementary particle collisions, Phys. Rev. **110**, 974 (1958).
[2] S. Weinberg, Infrared photons and gravitons, Phys. Rev. **140**, B516 (1965).
[3] V. N. Gribov, Bremsstrahlung of hadrons at high energies, Sov. J. Nucl. Phys. **5**, 280 (1967).
[4] T. H. Burnett and N. M. Kroll, Extension of the low soft photon theorem, Phys. Rev. Lett. **20**, 86 (1968).
[5] V. Del Duca, High-energy Bremsstrahlung theorems for soft photons, Nucl. Phys. **B345**, 369 (1990).
[6] B. Sahoo and A. Sen, Classical and quantum results on logarithmic terms in the soft theorem in four dimensions, J. High Energy Phys. 02 (2019) 086.
[7] H. Krishna and B. Sahoo, Universality of loop corrected soft theorems in 4d, J. High Energy Phys. 11 (2023) 233.
[8] W. Chen, M. x. Luo, T. Z. Yang, and H. X. Zhu, Soft theorem to three loops in QCD and $\mathcal{N}=4$ super Yang-Mills theory, J. High Energy Phys. 01 (2024) 131.
[9] F. Herzog, Y. Ma, B. Mistlberger, and A. Suresh, Single-soft emissions for amplitudes with two colored particles at three loops, J. High Energy Phys. 12 (2023) 023.
[10] A. Strominger, Lectures on the infrared structure of gravity and gauge theory, arXiv:1703.05448.
[11] G. F. Sterman, Partons, factorization and resummation, TASI 95, arXiv:hep-ph/9606312.
[12] A. H. Mueller, Asymptotic behavior of the Sudakov form-factor, Phys. Rev. D **20**, 2037 (1979).
[13] J. C. Collins, Algorithm to compute corrections to the Sudakov form-factor, Phys. Rev. D **22**, 1478 (1980).
[14] A. Sen, Asymptotic behavior of the Sudakov form-factor in QCD, Phys. Rev. D **24**, 3281 (1981).
[15] G. P. Korchemsky, Sudakov form-factor in QCD, Phys. Lett. B **220**, 629 (1989).
[16] L. J. Dixon, L. Magnea, and G. F. Sterman, Universal structure of subleading infrared poles in gauge theory amplitudes, J. High Energy Phys. 08 (2008) 022.
[17] I. Feige and M. D. Schwartz, Hard-soft-collinear factorization to all orders, Phys. Rev. D **90**, 105020 (2014).
[18] O. Erdoğan and G. Sterman, Ultraviolet divergences and factorization for coordinate-space amplitudes, Phys. Rev. D **91**, 065033 (2015).
[19] Y. Ma, A forest formula to subtract infrared singularities in amplitudes for wide-angle scattering, J. High Energy Phys. 05 (2020) 012.
[20] C. W. Bauer, D. Pirjol, and I. W. Stewart, Soft collinear factorization in effective field theory, Phys. Rev. D **65**, 054022 (2002).
[21] T. Becher, A. Broggio, and A. Ferroglia, Introduction to soft-collinear effective theory, Lect. Notes Phys. **896**, 1 (2015).
[22] V. S. Dotsenko and S. N. Vergeles, Renormalizability of phase factors in the nonAbelian gauge theory, Nucl. Phys. **B169**, 527 (1980).
[23] G. F. Sterman, Infrared divergences in perturbative QCD, AIP Conf. Proc. **74**, 22 (1981).
[24] S. Mukhi and G. F. Sterman, QCD jets to all logarithmic orders, Nucl. Phys. **B206**, 221 (1982).
[25] J. G. M. Gatheral, Exponentiation of eikonal cross-sections in nonAbelian gauge theories, Phys. Lett. **133B**, 90 (1983).
[26] J. Frenkel and J. C. Taylor, Nonabelian eikonal exponentiation Nucl. Phys. **B246**, 231 (1984).
[27] E. Laenen, G. Stavenga, and C. D. White, Path integral approach to eikonal and next-to-eikonal exponentiation, J. High Energy Phys. 03 (2009) 054.
[28] A. Mitov, G. Sterman, and I. Sung, Diagrammatic exponentiation for products of Wilson lines, Phys. Rev. D **82**, 096010 (2010).
[29] J. Frenkel, J. G. M. Gatheral, and J. C. Taylor, Quark-antiquark annihilation is infrared safe at high energy to all orders, Nucl. Phys. **B233**, 307 (1984).
[30] C. F. Berger, Higher orders in $A(\alpha_s)/[1-x]_+$ of nonsinglet partonic splitting functions, Phys. Rev. D **66**, 116002 (2002).
[31] G. F. Sterman, Zero mass limit for gauge singlet production amplitudes, Phys. Lett. **73B**, 440 (1978).
[32] E. V. Shuryak, The 'soft photon puzzle' and pion modification in hadronic matter, Phys. Lett. B **231**, 175 (1989).
[33] G. W. Botz, P. Haberl, and O. Nachtmann, Soft photons in hadron hadron collisions: Synchrotron radiation from the QCD vacuum?, Z. Phys. C **67**, 143 (1995).
[34] Y. Hatta and T. Ueda, Soft photon anomaly and gauge/string duality, Nucl. Phys. **B837**, 22 (2010).
[35] D. E. Kharzeev and F. Loshaj, Anomalous soft photon production from the induced currents in Dirac sea, Phys. Rev. D **89**, 074053 (2014).
[36] C. Y. Wong, An overview of the anomalous soft photons in hadron production, Proc. Sci. Photon192 (**2013**) 002.
[37] P. V. Chliapnikov *et al.* (Brussels-CERN-Genoa-Mons-Nijmegen-Serpukhov Collaborations), Observation of direct soft photon production in K^+p interactions at 70-GeV/c, Phys. Lett. **141B**, 276 (1984).
[38] S. Banerjee *et al.* (SOPHIE/WA83 Collaboration), Observation of direct soft photon production in $\pi^- p$ interactions at 280-GeV/c, Phys. Lett. B **305**, 182 (1993).
[39] J. Abdallah *et al.* (DELPHI Collaboration), Evidence for an excess of soft photons in hadronic decays of Z^0, Eur. Phys. J. C **47**, 273 (2006).
[40] Ø. Almelid, C. Duhr, and E. Gardi, Three-loop corrections to the soft anomalous dimension in multileg scattering, Phys. Rev. Lett. **117**, 172002 (2016).
[41] N. Agarwal, L. Magnea, C. Signorile-Signorile, and A. Tripathi, The infrared structure of perturbative gauge theories, Phys. Rep. **994**, 1 (2023).